Effect of TEA on the blue emission of ZnO quantum dots with high quantum yield

Jorge Oliva[1], Luis Diaz-Torres[1], Alejandro Torres-Castro[2], Pedro Salas[3], Leonardo Perez-Mayen[1] and Elder De la Rosa[1]*

[1]Centro de Investigaciones en Optica, A.P. 1-948, León, Gto. 37160 México
[2]Universidad Autónoma de Nuevo León, A.P. 126-F, Monterrey, Nuevo León, 66450 México
[3]Centro de de Fisica Aplicada y Tecnología Avanzada, UNAM, Queretaro, Qro., México
**elder@cio.mx*

Abstract: This work reports the luminescence, morphology and synthesis of ZnO quantum dots using a simple wet chemical method and different concentrations of Triethanolamine (TEA) as surfactant. Those nanoparticles emitted a strong blue emission band centered at 429 nm when they are dispersed in hexane. Spherical quantum dots with sizes ranging from 3 to 7 nm were obtained for concentrations from 0 to 0.7 ml. of TEA, whereas a mixture with oval-like nanoparticles was observed from concentrations above of 1.1 ml of TEA. It was also possible to control the values of the band gap in ZnO quantum dots depending on the content of TEA. Based on the high quantum yield of 81% measured for those ZnO nanoparticles respect to quinine sulfate dye (QS), it is suggested that such nanoparticles could be used for biolabeling and ZnO based LEDs.

©2015 Optical Society of America

OCIS codes: (160.0160) Materials; (300.0300) Spectroscopy; (160.4236) Nanomaterials; (160.4760) Optical properties.

References and links

1. R. Gopikrishnan, K. Zhang, P. Ravichandran, S. Baluchamy, V. Ramesh, V. Biradar, P. Ramesh, J. Pradhan, J. C. Hall, A. K. Pradhan, and G. T. Ramesh, "Synthesis, characterization and biocompatibility Studies of Zinc oxide (ZnO) nanorods for biomedical application," Nano-Micro Letters **2**(1), 31–36 (2010).
2. D. J. Rogers, F. H. Teherani, V. E. Sandana, and M. Razeghi, "ZnO thin films and nanostructures for emerging optoelectronic applications," Proc. SPIE **7605**, 76050K(2010).
3. D. Weber, S. Botnaraş, D. V. Pham, J. Steigerb, and L. De Colac, "Functionalized ZnO nanoparticles for thin-film transistors: support of ligand removal by non-thermal methods," J. Mater. Chem. C **1**(18), 3098–3103 (2013).
4. S. Peng, G. Wu, W. Song, and Q. Wang, "Application of flower-like ZnO nanorods gas sensor detecting SF6 decomposition products," J. Nanomater. **2013**, 135147 (2013).
5. Z. Longyue, D. Songyuan, X. Weiwei, and W. Kongjia, "Dye-sensitized solar cells based on ZnO films," Plasma Sci. Technol. **8**(2), 172–175 (2006).
6. Z. Zang, A. Nakamura, and J. Temmyo, "Single cuprous oxide films synthesized by radical oxidation at low temperature for PV application," Opt. Express **21**(9), 11448–11456 (2013).
7. J. You, L. Dou, K. Yoshimura, T. Kato, K. Ohya, T. Moriarty, K. Emery, C. C. Chen, J. Gao, G. Li, and Y. Yang, "A polymer tandem solar cell with 10.6% power conversion efficiency," Nat. Commun. **4**, 1446 (2013).
8. A. Pang, C. Chen, L. Chen, W. Liu, and M. Wei, "Flexible dye-sensitized ZnO quantum dots solar cells," RSC Advances **2**(25), 9565–9570 (2012).
9. E. De la Rosa, S. Sepúlveda-Guzman, B. Reeja-Jayan, A. Torres, P. Salas, N. Elizondo, and M. Jose Yacaman, "Controlling the growth and luminescence properties of well-Faceted ZnO nanorods," J. Phys. Chem. C **111**(24), 8489–8495 (2007).
10. Y. Yang, X. W. Sun, B. K. Tay, P. H. T. Cao, J. X. Wang, and X. H. Zhang, "Revealing the surface origin of green band emission from ZnO nanostructures by plasma immersion ion implantation induced quenching," J. Appl. Phys. **103**(6), 064307 (2008).
11. V. Kumar, H. C. Swart, O. M. N. Twaeaborwa, R. E. Kroon, J. J. Terblans, S. K. K. Shaat, A. Yousif, and M. M. Duvenhage, "Origin of the red emisión in zinc oxide nanophosphors," Mater. Lett. **101**, 57–60 (2013).
12. A. B. Djuriši, Y. H. Leung, K. H. Tam, L. Ding, W. K. Ge, H. Y. Chen, and S. Gwo, "Green, yellow, and orange defect emission from ZnO nanostructures: Influence of excitation wavelength," Appl. Phys. Lett. **88**(10), 103107 (2006).
13. G. H. Du, F. Xu, Z. Y. Yuan, and G. V. Tendeloo, "Flowerlike ZnO nanocones and nanowires: preparation, structure, and luminescence," Appl. Phys. Lett. **88**(24), 243101 (2006).

#232086 - $15.00 USD Received 16 Jan 2015; revised 30 Mar 2015; accepted 5 Apr 2015; published 17 Apr 2015

14. D. H. Zhang, Z. Y. Xue, and Q. P. Wang, "The mechanisms of blue emission from ZnO films deposited on glass substrate by r.f. magnetron sputtering," J. Phys. D Appl. Phys. **35**(21), 2837–2840 (2002).
15. Z. Zulkifli, S. Munisamy, M. Z. M. Yusop, G. Kalita, and M. Tanemura, "Fabrication of nanostructured ZnO films for transparent field emission displays," Jpn. J. Appl. Phys. **52**(11S), 11NJ07 (2013).
16. Y. He, J. A. Wang, X. B. Chen, W. F. Zhang, X. Y. Zeng, and Q. W. Gu, "Blue electroluminescence Nanodevice prototype based on vertical ZnOnnanowire/polymer film on silicon substrate," J. Nanopart. Res. **12**(1), 169–176 (2010).
17. Z. Shi, Y. Zhang, J. Zhang, H. Wang, B. Wu, X. Cai, X. Cui, X. Dong, H. Liang, B. Zhang, and G. Du, "High-performance ultraviolet-blue light-emitting diodes based on an n-ZnO nanowall networks/p-GaN heterojunction," Appl. Phys. Lett. **103**(2), 021109 (2013).
18. J. Chen, D. Zhao, C. Li, F. Xu, W. Lei, L. Sun, A. Nathan, and X. W. Sun, "All solution-processed stable white quantum dot light-emitting diodes with hybrid ZnO@TiO as blue emitters," Sci Rep **4**, 4085 (2014).
19. Z. Zang and X. Tang, "Enhanced fluorescence imaging performance of hydrophobic colloidal ZnO nanoparticles by a facile method," J. Alloys Compd. **619**, 98–101 (2015).
20. Y. S. Fu, X. W. Du, S. A. Kulinich, J. S. Qiu, W. J. Qin, R. Li, J. Sun, and J. Liu, "Stable Aqueous Dispersion of ZnO Quantum Dots with Strong Blue Emission via Simple Solution route," J. Am. Chem. Soc. **129**(51), 16029–16033 (2007).
21. B. Efafi, M. S. Ghamsari, M. A. Aberoumand, M. H. M. Ara, and H. H. Rad, "Highly concentrated ZnO sol with ultra-strong green emission," Mater. Lett. **111**, 78–80 (2013).
22. S. K. Mishraa, S. Bayana, R. Shankar, P. Chakraborty, and R. K. Srivastava, "Efficient UV photosensitive and photoluminescence properties of sol–gel derived Sn doped ZnO nanostructures," Sens. Actuators A Phys. **211**, 8–14 (2014).
23. Q. Yue, J. Cheng, G. Li, K. Zhang, Y. Zhai, L. Wang, and J. Liu, "Fluorescence property of ZnO nanoparticles and the interaction with bromothymol blue," J. Fluoresc. **21**(3), 1131–1135 (2011).
24. S. Gulia and R. Kakkar, "ZnO quantum dots for biomedical applications," Adv. Mat. Lett. **4**(12), 876–887 (2013).
25. P. Felbier, J. Yang, J. Theis, R. W. Liptak, A. Wagner, A. Lorke, G. Bacher, and U. Kortshage, "Highly Luminescent ZnO Quantum Dots Made in a Nonthermal Plasma," Adv. Funct. Mater. **24**(14), 1988–1993 (2014).
26. L. W. Sun, H. Q. Shi, W. N. Li, H. M. Xiao, S. Y. Fu, X. Z. Cao, and Z. X. Li, "Lanthanum-doped ZnO quantum dots with greatly enhanced fluorescent quantum yield," J. Mater. Chem. **22**(17), 8221–8227 (2012).
27. H. M. Xiong, Z. D. Wang, and Y. Y. Xia, "Polymerization initiated by inherent free radicals on nanoparticle surfaces: a simple method of obtaining ultrastable (ZnO)polymer core–shell nanoparticles with strong blue fluorescence," Adv. Mater. **18**(6), 748–751 (2006).
28. R. Yogamalar, R. Srinivasan, and A. C. Bose, "Multi-capping agents in size confinement of ZnO nanostructured particles," Opt. Mater. **31**(11), 1570–1574 (2009).
29. M. L. Singla, M. Shafeeq, and M. M. Kumar, "Optical characterization of ZnO nanoparticles capped with various surfactants," J. Lumin. **129**(5), 434–438 (2009).
30. B. Tang, B. Zhou, J. Zhao, X. Lv, F. Sun, and Z. Wang, "Synthesis of morphological ZnO particles by a facile solution-based chemical method," Colloids Surf. A Physicochem. Eng. Asp. **332**(1), 43–49 (2009).
31. K. Thongsuriwong, P. Amornpitoksuk, and S. Suwanboon, "The effect of aminoalcohols (MEA, DEA and TEA) on morphological control of nanocrystalline ZnO powders and its optical properties," J. Phys. Chem. Solids **71**(5), 730–734 (2010).
32. J. W. P. Hsu, D. R. Tallant, R. L. Simpson, N. A. Missert, and R. G. Copeland, "Luminescent properties of solution-grown ZnO nanorods," Appl. Phys. Lett. **88**(25), 252103 (2006).
33. M. A. Bakar, M. A. A. Hamid, and A. Jalar, "Growth behavior of ZnO on Si (100) and platinum coated glass substrate from aqueous solution," Adv. Mat. Res. **97-101**, 1550–1553 (2010).
34. M. S. Mamat, Z. Khusaimi, and M. R. Mahamood, "Growth of multi-shaped zinc oxide nanostructures using C-axis oriented zinc oxide thin films as a seeded catalyst via hydrothermal aqueous chemical growth method," Defect and Difusion Forum. **312–315**, 1126–1131 (2011).
35. Y. Gu, I. L. Kuskovsky, M. Yin, S. O'Brien, and G. F. Neumark, "Quantum confinement in ZnO nanorods," Appl. Phys. Lett. **85**(17), 3833 (2004).
36. H. Zheng, G. Duan, Y. Li, S. Yang, X. Xu, and W. Cai, "Blue luminescence of ZnO nanoparticles based on non-equilibrium processes: defect origins and emission controls," Adv. Funct. Mater. **20**(4), 561–572 (2010).
37. Z. Fang, Y. Wang, D. Xu, Y. Tan, and X. Liu, "Blue luminescent center in ZnO films deposited on silicon substrates," Opt. Mater. **26**(3), 239–242 (2004).
38. M. K. Patra, M. Manoth, V. K. Singh, G. S. Gowd, V. S. Choudhry, S. R. Vadera, and N. Kumar, "Synthesis of stable dispersion of ZnO quantum dots in aqueous medium showing visible emission from bluish green to yellow," J. Lumin. **129**(3), 320–324 (2009).
39. A. Goldeblum, A. Belum-Marian, and V. Teodorescu, "Optical properties of ZnO nanocrystallites embedded in a gold-oxide matrix," J. of Opt. and Adv. Mat. **8**(6), 2129–2132 (2006).
40. Z. W. Donga, C. F. Zhang, H. Deng, G. J. You, and S. X. Qian, "Raman spectra of single micrometer-sized tubular ZnO," Mater. Chem. Phys. **99**(1), 160–163 (2006).
41. C. A. J. Lin, T. Y. Yang, C. H. Lee, S. H. Huang, R. A. Sperling, M. Zanella, J. K. Li, J. L. Shen, H. H. Wang, H. I. Yeh, W. J. Parak, and W. H. Chang, "Synthesis, characterization, and bioconjugation of fluorescent gold nanoclusters toward biological labeling applications," ACS Nano **3**(2), 395–401 (2009).

#232086 - $15.00 USD Received 16 Jan 2015; revised 30 Mar 2015; accepted 5 Apr 2015; published 17 Apr 2015
(C) 2015 OSA

1. Introduction

ZnO nanoparticles are an important topic of research due to their applications in different areas such as biological systems, optoelectronics devices such as LEDs, solar cells, and gas sensors just to mention a few [1–8]. ZnO has a room temperature bandgap of 3.37 eV and a large excitonic (electron-hole) binding energy of 60 meV, larger than thermal energy at room temperature (26 meV) [9]. The characteristic emission band of ZnO is centered at 390 nm and is attributed to the free excitons recombination. Green (520 nm), yellow and orange (620 nm) emission bands have been reported in both nano- and bulk ZnO crystals. The green one has been related to the amount of oxygen deficiency or oxygen vacancies, while the yellow and orange emissions are associated with an excess of oxygen [9–12]. Blue emission has been reported and ascribed to electron transition from shallow donor level of oxygen vacancies (ΔE_g = ~2.8 eV) and zinc interstitial (ΔE_g = ~2.7eV) to the valence band [13,14]. Both, oxygen vacancies and zinc interstitial, were probably formed during the synthesis process due to the reaction parameters such as time, solvent and temperature. Those visible emission bands make ZnO a very attractive low-voltage phosphor for field emission displays [15]. The improvement of the quantum yield (QY) in ZnO for the blue region is important for the fabrication of efficient white and blue emitting ZnO based LEDs, as well as for biolabeling [16–19]. Recently, strong blue emission was reported and suggested to arise from the formation of surface ZnO/oleic acid (OA) complexes formed when hydroxyl groups coming from diethanolamine (DEA) reacts with carboxyl groups from oleic acid [20]. Several groups have made efforts to increase the luminance of ZnO nanoparticles in the green and blue regions by introducing dopants such as Sn or by modification of the ZnO by sol-gel process [21,22]. Some groups have reported values of QY around 45%, 21% and 60% for green, blue and yellow emissions respectively, and those values were obtained using the QY of a dye as reference [23–25]. More recently, efficiencies as high as 78% for green emission was reported for La-doped ZnO [26]. Furthermore, surface treatments of ZnO nanoparticles with polymers such as PMMA or PMAA was performed to increase the QY up to 80% for blue emission [27]. However, those (ZnO)PMAA-PMMA colloids would not be useful for the fabrication of ZnO based LEDs or optoelectronic devices due to the isolating properties of PMMA. All defects responsible of visible emission are produced during the synthesis processes, but in general, their presence as well as their density are not fully controlled. Furthermore, those defects can change from one batch to another one. Thus, controlling the synthesis process in order to select and control the presence of specific defects is a challenge, and this is a very important subject of research around the world.

Research groups have been working to control size, morphology, photoluminescence (PL) and the energy band gap (BG) of ZnO. Various surfactant and capping agents has been used to obtain particles with sizes ranging from 10 to 25 nm and BG ~3.86 to 4 eV [28,29]. The use of oleic acid not only induce surface defect associated to blue emission but also control the size and morphology of nanocrystals [20]. Recently, Triethanolamine (TEA) has been used to control the size and morphology of ZnO nanoparticles, the sizes are ranging from 3 to 75 nm and the morphologies are spheres, rugby-like, rice-like and nanorods, and the BG for those morphologies are ranging from 3.27 to 3.94 eV. Those changes in shape are possible because TEA permits the formation of stable complexes such as $Zn(OH)_2$ and $Zn(OH)_4^{-2}$ which act as growth units [30,31]. Thus, TEA could be useful as capping agent in ZnO nanoparticles and as modifier of morphology. It could be more advantageous using TEA as surfactant to produce blue light instead of OA, since the last one needs to be combined with other compounds such as DEA to form carboxylate groups on the surface of ZnO nanocrystals which in turn create defects for blue emission [20]. To the best of our knowledge, it has not been reported a systematic study of the effect of TEA on the blue emission of ZnO nanoparticles, therefore, we present in this work a simple method to synthesize ZnO quantum dots (QDs) using only TEA as surfactant. Different concentrations of TEA introduced during the synthesis of ZnO QDs allowed us to control their size, band gap and intensity of blue emission. The sample with the highest blue emission had a quantum

#232086 - $15.00 USD Received 16 Jan 2015; revised 30 Mar 2015; accepted 5 Apr 2015; published 17 Apr 2015
(C) 2015 OSA

yield of 81% when it is dispersed in hexane. Our method of synthesis was simple and we did not use rare earths as dopants or insulating polymers to reach a high QY. Hence, the results presented in this work indicate that our ZnO quantum dots would be useful to fabricate biolabels and optoelectronic devices such as ZnO based LEDs.

2. Experimental details

2.1 Synthesis procedure

All reagents and surfactants with a purity of at least 98% were acquired from Sigma Aldrich and were used without further purification. ZnO quantum dots were synthesized from an alcohol based solution. This solution was prepared by mixing 10 gr. of Zinc acetate ($Zn(O_2CCH_3)_2(H_2O)_2$, ZnAc) and 40 ml of methanol, later, water was added in such a way that a $ZnAc/H_2O$ molar ratio of 0.2 was reached, and Triethanolamine ($C_6H_{15}NO_3$, TEA) was added. This reaction mixture was stirred at 60 °C during 1h. Subsequently, hexane was introduced to produce precipitation. Afterwards, the white powder was separated by centrifugation, washed several times with methanol and dried at 100°C during 1h. Five samples were prepared with different concentrations of TEA: 0, 0.5, 0.7, 1.1 and 1.8 ml and named as T0, T1, T2, T3 and T4 respectively. Two additional samples were prepared with similar conditions but zinc nitrate and hydroxylamine were used as source of Zn and as surfactant respectively, such samples are identified as T5, and T6. Other samples T7 and T8 were prepared by using the same synthesis conditions of T3, but sample T7 was fabricated using oleic acid as capping agent and sample T8 employed sodium hydroxide as precipitant agent instead of hexane.

2.2 Structural and morphological characterization

Morphology and crystalline characterization of the samples were performed in a High Resolution Transmission Electron Microscopy (HRTEM), FEI- Titan 80-300 KeV. The microscope is equipped with Ultra stable Schottky field emitter gun. The samples were grounded, suspended in isopropanol at room temperature, and dispersed with ultrasonic agitation; then, an aliquot of the solution was dropped on a 3mm diameter lacey carbon copper grid for examination. The crystalline phase of ZnO QDs was obtained by x-ray powder diffraction using a Siemens D-5005 diffractometer with a Cu tube and Kα radiation at 1.5405 Å, scanning in the 15°– 80° range (2θ) with increments of 0.02° and a sweep time of 2 s.

2.3 Optical characterization

Photoluminescence spectra were obtained under 350 nm excitation from a Xenon Lamp (Acton Research Corporation) of 75 Watts. The fluorescence emission was analyzed with an Acton Pro 3500i monochromator and a R955 Hamamatsu photomultiplier tube for visible emission. All samples were dispersed in hexane for PL measurements. The absorption spectra ranging from 200 to 800 nm were obtained from a Perkin Elmer lambda 900 spectrometer and using a 1 cm quartz cell. The IR spectra [Fourier transform infrared (FTIR)] of samples were recorded in the range of 400–4000 cm^{-1} on an ABA (MB300) spectrometer using the KBr pellet method. The quantum yield (QY) of ZnO quantum dots emitting blue light was calculated by using quinine sulfate dye (QS) as a reference according to the procedure explained in section 3.5. All optical measurements were done at room temperature.

3. Results and discussion

3.1 Effect of TEA on the Structure and Morphology of ZnO quantum dots

HRTEM images in Fig. 1(a) and 1(b) show that ZnO nanoparticles are spheres for concentrations of TEA below 0.7 ml. (samples T0, T1 and T2), while oval-like nanoparticles mixed with spherical nanoparticles appeared for concentrations above 1.1 ml. of TEA (samples T3 and T4), see Fig. 1(c) and 1(d). Those ZnO nanoparticles correspond to the

#232086 - $15.00 USD Received 16 Jan 2015; revised 30 Mar 2015; accepted 5 Apr 2015; published 17 Apr 2015
(C) 2015 OSA

spatial group $P6_3mc$ (186) with cell parameters a = 3.2494 Å and c = 5.2038 Å. In addition, the FFT in inset of Fig. 1(b) shows the (00-2), (002), (10-2), (10-1), (100), and (200) planes corresponding to hexagonal structure, according to the 36-1451 JCPDS card.

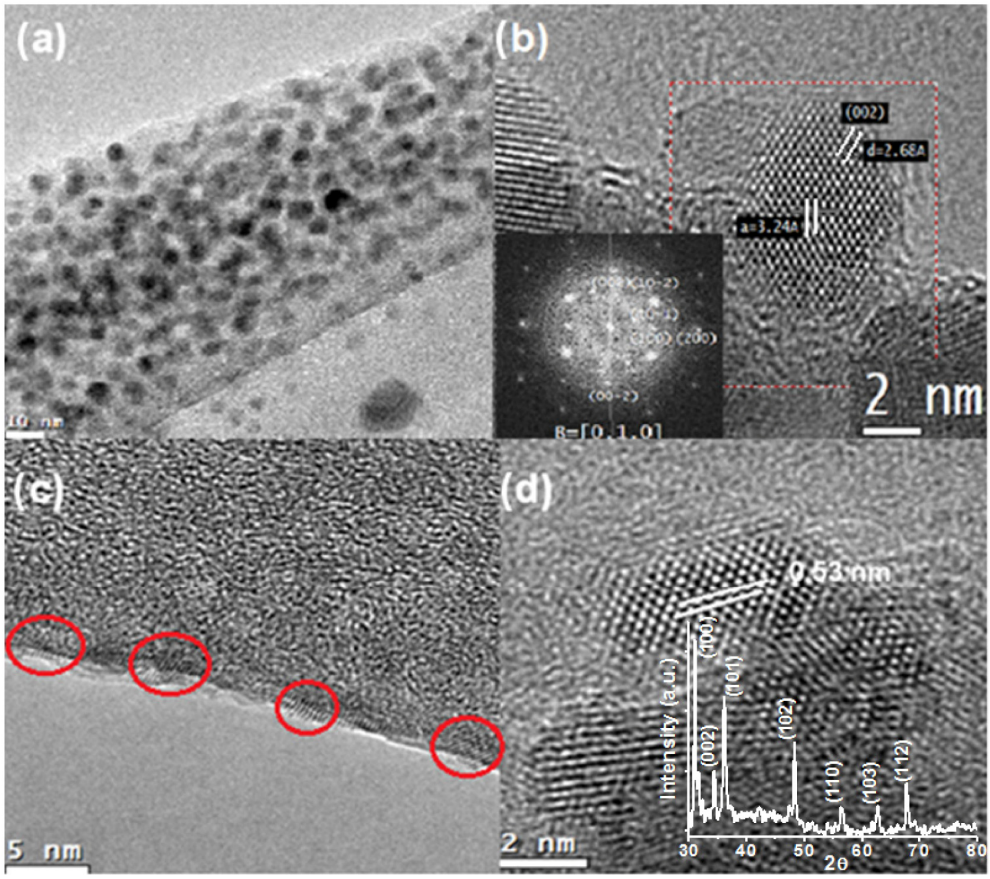

Fig. 1. HRTEM images of ZnO quantum dots: (a) and (b) correspond to sample T2 (0.7 ml of TEA), (c) and (d) correspond to sample T3 (1.1 ml. of TEA). Insets in Figs. 1(b) and 1(d) show the FFT transform of spherical nanoparticles with their corresponding crystalline planes and the XRD spectrum of sample T2 respectively.

By comparing Figs. 1(b) and 1(d), we observed that the distance between crystalline planes increased from 0.324 nm to 0.53 nm, this could be due to the enlargement from spherical nanoparticles to oval-like nanoparticles as consequence of increasing the amount TEA during the process of synthesis. Spheres in Fig. 1(b) corresponding to sample T2 have an average diameter of 4.1 ± 0.4 nm, and oval-like nanoparticles in Fig. 1(d) presented an average length and diameter of 5.5 ± 0.4 nm and 1.8 ± 0.2 nm respectively. Table 1 shows the values of average size of spheres and oval-like nanoparticles corresponding to each concentration of TEA. In general, it is observed that the size of spherical nanocrystals increases from 3.5 nm to 6.5 nm as the amount of TEA increases. In addition, the change from spheres to oval-like nanoparticles could be explained taking into account that TEA is a capping agent very effective to inhibit the growth of nanoparticles along the c-axis [31].

Also the steric effect, that is, repulsive forces among molecules of the same type, occur predominantly in TEA, thus, this effect should increase as the content of TEA increases. Therefore, after certain concentration of TEA (1.1 ml.), only a lateral growth of quantum dots is allowed along the a-axis to stabilize the ZnO nanoparticles [32], giving raise to oval-like morphology. If the amount of TEA is increased up to 1.8 ml (sample T4), the average length

#232086 - $15.00 USD Received 16 Jan 2015; revised 30 Mar 2015; accepted 5 Apr 2015; published 17 Apr 2015
(C) 2015 OSA

of oval-like nanoparticles increases from 5.5 nm to 7.5 nm because the surface of ZnO nanoparticles is saturated with TEA after 1.1 ml, which avoids a growth of nanoparticles in any direction, Then, the Ostwald ripening could occur to form larger nanoparticles with shape of ovals due to the coalescence of the small ones. To the best of our knowledge, we are reporting for the first time oval-like nanoparticles of ZnO with sizes less than 10 nm, other authors such as M.A. Bakar et al. and M. Mamat have reported oval-like nanoparticles above 10 nm and they used hexamethylenetretamine as surfactant [33,34].

Finally, the inset in Fig. 1(d) shows the XRD spectrum of sample T2 (0.7 ml. TEA). The planes (100), (002), (101), (102), (110), (103) and (112) are associated to the wurtzite structure of ZnO according to JCPDS 36-1451 card. The crystalline phase of the ZnO nanoparticles did not change with the increase of TEA concentration, suggesting that our method of synthesis can produce nanoparticles with stable structure. The samples with a mixture of morphologies (T3 and T4) also had the same wurtzite structure (not showed here), indicating that both, spheres and oval-like nanoparticles have the same phase.

Table 1. Synthesis parameters of samples T0-T4 and energy band gap calculations.

	TEA (ml.)	UV absorption Peak (nm)	Average Size (nm) ±0.4nm	Energy Band Gap (eV)	Effective mass Approx. (eV)	Shape	T(^{0}C)
T0	0	269	3.5	4.15	4.08	Spheres	60
T1	0.5	273	4.3	4.03	3.81	Spheres	60
T2	0.7	271	4.1	4.06	3.86	Spheres	60
T3	1.1	274	4.5(spheres) 5.5 (oval-like)	3.98	3.76	Spheres and oval-like	60
T4	1.8	279	6.5 (spheres), 7.5 (oval-like)	3.82	3.55	Spheres and oval-like	60

3.2 Effect of TEA on the Absorption and Band Gap of ZnO quantum dots

The optical energy band gap (BG) of the samples T0-T4 was calculated in two different ways: By using an extrapolating method (Tauc approach) which requires the absorption spectra of ZnO nanoparticles and by using the equation of effective mass approximation [20,28].

Figures 2(a) and 2(b) show the absorption bands and the extrapolation of the linear part (see dotted lines) in the $(\alpha h\nu)^2$ vs $h\nu$ curves of samples T0-T2 respectively. Basically, the intersection of the dotted lines with the $h\nu$ axis gives the optical energy band gap value. According to the results of energy band gap in Table 1, the values of BG obtained with both methods were similar; the highest difference between those values was 7% taking as reference the values of energy band gap obtained using the extrapolating method, indicating that our calculations are consistent and with good accuracy. Also, Table 1 shows that the absorption peaks of the samples T0-T4 shift to higher wavelengths (excepting T2) as the amount of TEA increases (the absorption band of sample T1 is centered at about 273 nm). Furthermore, the size of nanoparticles increases sucessively in samples T0 to T4 while their energy gap values decreases at the same time (we are omitting for this trend sample T2). Thus, as the content of TEA decreases the quantum confinement effect is favored because the size of nanoparticles is near of the bulk exciton bohr radius a_B = 2.34 nm, that is, the reduction of the energy band gap by increasing size of nanoparticles will be approaching to the value of 3.37 eV for the bulk in ZnO. This decrease in the BG as the size of nanoparticles increases is in agreement with reported literature [31]. However, results for sample T2 are not in agreement with the trend of quantum confinement, this difference could be caused by the

#232086 - $15.00 USD Received 16 Jan 2015; revised 30 Mar 2015; accepted 5 Apr 2015; published 17 Apr 2015
(C) 2015 OSA

"sharpeness" of the absorption band for this sample. The absorption bands of the other samples are broad, see Fig. 2(a), but the absorption of T2 is not very broad in comparison to the other samples. When we draw an imaginary line on the curve of $(\alpha h\nu)^2$ versus $h\nu$ for this sample T2 (see green dotted line), this line has a higher slope, which in turn, will produce an intersection at higher energies on the x-axis (compared with T1). In the case of samples T3 and T4 which contain a mixture of spherical and oval-like nanoparticles, an increase in TEA produces lower BG values. This reduction could be explained considering that a higher concentration of TEA increases the average length of oval-like nanoparticles, from 5.5 nm (sample T3) to 7.5 nm (sample T4), this in turn shifts the absorption band to longer wavelengths, therefore, the value of BG decreased. It is worthy to notice that the BG values of spheres and oval-like are higher than these reported by other authors [20,28,31]. This could be explained taking into account that the sizes of the spheres, see Table 1, are near to the value of 2.34 nm, corresponding to the exciton Bohr radius of ZnO bulk, in consequence, spherical ZnO quantum dots present strong confinement effects. Further, ZnO oval-like nanoparticles also present strong confinement effects because their average diameter is below 2 nm [35], as result their BG values are higher. Finally, it has been reported energy band gap values around 4 eV wih sizes ranging from 17 to 25 nm, this suggests that our results are reliable because we have lower nanoparticles sizes [28].

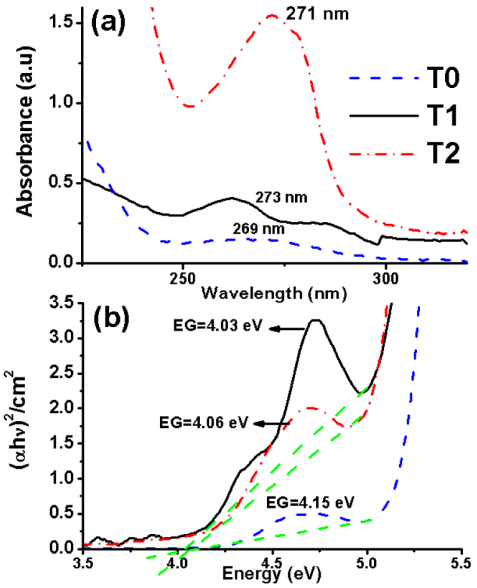

Fig. 2. (a) UV absorption bands of samples T0-T2 and (b) $(\alpha h\nu)^2$ vs. $h\nu$ curves for calculation of optical Band Gap in samples T0-T2.

3.3 Effect of TEA on the Luminescence of ZnO quantum dots

The photoluminescence (PL) and photoluminescence excitation (PLE) spectra of samples T0 (synthesized without TEA) and T3 (synthesized with TEA) are shown in Fig. 3(a). Both samples presented a blue emission band centered at 429 nm (2.89 eV) under 350 nm excitation, but the overall emission of sample T0 was 7.5 times lower. This blue emission is depicted in the inset of Fig. 3(a). In order to identify the origin of the blue emission, it is convenient to make a deconvolution of the emission spectrum. This will permit us to distinguish each component (gaussian components) of the emission band centered at 429 nm. As observed, such spectrum is the result of the overlapping of gaussian curves centered at 405

#232086 - $15.00 USD Received 16 Jan 2015; revised 30 Mar 2015; accepted 5 Apr 2015; published 17 Apr 2015
(C) 2015 OSA

nm, 429 nm and 453 nm and 475 nm, each one associated to the shoulder observed in the emission spectrum, see Fig. 3(b). According to literature, each of these blue emissions are caused by zinc interstitial defects, in consequence, we can confirm that the origin of the blue emission observed in this work is originated from this type of defects [13,14].

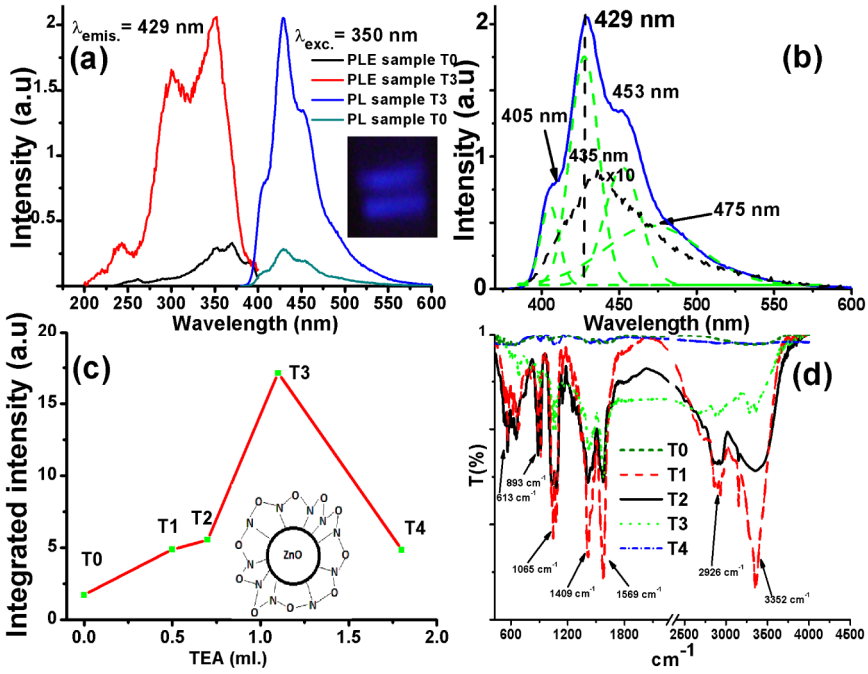

Fig. 3. (a) PL and PLE spectra of samples T0 and T3 without/with TEA, (b) PL spectra of sample T3 dispersed in hexane and methanol with Gaussian fitting, (c) Integrated photoluminescence as function of TEA concentration and (d) FTIR spectra of samples T0-T4 prepared with different concentrations of TEA. Insets in Figs. 3(a) and 3(c) show a photograph of blue emission produced in ZnO nanoparticles and the polymeric capping around ZnO QDs respectively.

The shape of the blue emission band centered at 429 nm did not change regardless an increase in the amount of TEA, indicating that other type of defect (oxygen vacancies, zinc vacancies etc.) are not formed when the content of TEA is increased. If those defects appear, green or yellow emissions should be observed, but it did not occur; thus, defects that produce emission peaks at 405 nm, 429 nm, 453 nm and 475 nm are stable. The structure of the photoluminescence spectrum of the sample T3 was identical to those of the samples T1, T2 and T4 (not showed here). Those spectra did not show UV emission at 390 nm (associated to the energy gap of ZnO) under excitation at 350 nm due to a "screening effect" of the blue emission. The surface of ZnO nanocrystals is rather excited instead of the "bulk" of the nanocrystals with better crystallinity which can produce 390 nm emission, as result, the blue emission is mainly favored (defects that originate the blue emission are located on the surface of ZnO QDs). Furthermore, it is observed that the PLE spectrum of the sample T3 has an extra band centered at 300 nm in comparison with the excitation spectra of the sample T0, see Fig. 3(a). A higher emission intensity induced by the introduction of TEA (in sample T3 respect to T0) and an additional excitation band, suggest that the presence of TEA increases the amount of surface states (defects) by bonding TEA molecules on the surface of ZnO quantum dots. In consequence, the blue emission increases as the content of TEA increases, see Fig. 3(c).

The presence of TEA on the surface of ZnO nanoparticles in samples T1-T4 was detected by FTIR measurements as depicted in Fig. 3(d), see the bands centered at 2926 cm^{-1},

#232086 - $15.00 USD Received 16 Jan 2015; revised 30 Mar 2015; accepted 5 Apr 2015; published 17 Apr 2015
(C) 2015 OSA

1065cm^{-1}, 893 cm^{-1} and 613 cm^{-1} which are associated to TEA. Evidently, sample T0 did not show the presence of TEA. This effect of increasing defects as the amount of TEA increases is opposite to that affirmed by M.L. Singla et al. who reported that the presence of surfactants on the surface of ZnO nanocrystals decreases the amount of defects that produce visible emission [29]. The chemical bond between the molecule of TEA and the surface of ZnO could be caused by OH groups and amines coming from TEA. Therefore, the amine can remain on the surface of ZnO, which interacts with the Zinc or Oxygen atoms in the surface of nanocrystals. This can produce Zn interstitials or Zinc vacancies, which originate blue emission [36–38]. In fact, Zn interstitial defects are formed in Zn rich vapor environments and our synthesis procedure involved vapors coming from methanol boiling at 60°C and we used Zinc acetate as precursor [38]. The formation of defects due to the presence of TEA can be confirmed from the Raman spectra in Fig. 4. This graphic shows the $A_1(L0)$ and $E_1(LO)$ modes located in the 540-680 cm^{-1} range as well as other multiphononic lines such as 747 cm^{-1}, 866 cm^{-1}, 938 cm^{-1}, 1027 cm^{-1} and 1078 cm^{-1} corresponding to ZnO wurtzite structure [39,40].

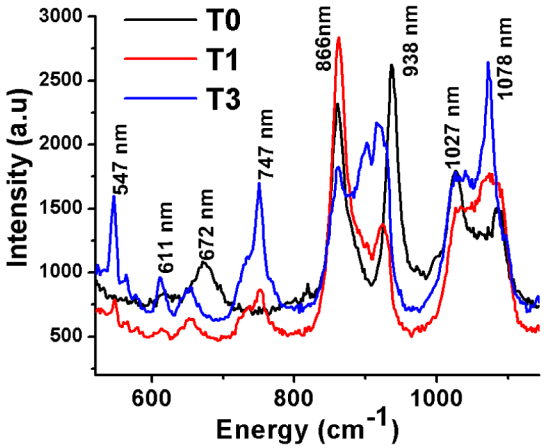

Fig. 4. Raman spectra of samples T0, T1 and T3.

By comparing the Raman Spectra of the samples T1 and T3 with that for T0, it is observed that the peaks related with the ZnO wurtzite structure and centered at 547 cm^{-1} and 747 cm^{-1} only appeared for samples T1 and T3. Also, the intensity of the peak at 1027 cm^{-1} decreased in sample T1 and T3 (which had TEA) compared to T0. Those results suggest that other Zn-O bonds are favored with the presence of TEA, and this means that atomic rearrangements of the crystalline lattice occurred, this in turn, can produce Zinc interstitial defects related with blue emission. Figure 3(c) shows that the integrated intensity for blue emission increases as the concentration of TEA increases, reaching a maximum for a concentration of 1.1 ml. and then decreases. This increase in luminescence with the content of TEA could be explained by taking into account that the amount of impurities, such as OHs (3352 cm^{-1} band) that quench luminescence in ZnO quantum dots, decreases as the amount of TEA increases, see FTIR spectra in Fig. 3(d). To better understand the effect of OH groups on the luminescent properties of ZnO nanoparticles dispersed in hexane, we measured the photoluminescence of ZnO quantum dots dispersed in methanol. As observed on the black curve in Fig. 3(b) (zoomed 10 times), the blue emission was quenched 95%, indicating that the presence of OHs decreases the luminescence. When ZnO QDs are dispersed in methanol the OH groups in this medium are linked to OH groups that are capping the ZnO nanoparticles, reducing the surface states that produce blue emission. Nevertheless, if ZnO nanoparticles are dispersed in a hydrophobic medium like hexane (C_6H_{15}), they are dispersed

#232086 - $15.00 USD Received 16 Jan 2015; revised 30 Mar 2015; accepted 5 Apr 2015; published 17 Apr 2015
(C) 2015 OSA

due to the steric effect. This avoids linking with OH groups (not present in hexane) and preserves the surface states that produce blue light. Hence, OH groups acting as capping agent around nanoparticles favor blue emission when ZnO quantum dots are dispersed in a hydrophobic medium as hexane, and are detrimental for emission when they are dispersed in a hydrophilic medium such as methanol.

The integrated blue emission of the sample T4 is lower than that for T3, suggesting that after certain concentration of TEA more defects cannot be formed in such way that emission would increase. If we continue adding TEA after a concentration of 1.1 ml, the polymeric capping formed with the OH groups and amines coming from TEA will increase in such a way that it would decrease the luminescence of nanoparticles, see inset in Fig. 3(c). This polymeric capping could be formed in the following way: 1) From a concentration of TEA of 0.5 ml, ammine and OH groups are linked to the surface of ZnO forming Zn interstitial defects, 2) if we increase the amount of TEA (concentrations of 0.7 and 1.1 ml.), several OHs react to release H_2O and at the same time a complex network, i.e. oxygen bridges between ammines (polymeric capping) are formed, see inset in Fig. 3(c). This produces a diminution of the amount of OH groups and in consequence, TEA molecules on the surface of ZnO also decreases, see FTIR spectra in Fig. 3(d), this in turn, produces an enhancement of the blue emission coming from defects. 3) If we continue increasing the content of TEA (1.8 ml), the surface of ZnO nanocrystals is over-saturated with TEA and the thickness of capping should increase, thus, the surface of ZnO nanoparticles should have a high amount of impurities but there are not bands related with TEA or OH groups as observed in Fig. 3(d). Probably the OH radicals reacted efficiently to form water when the content of TEA was very high, in consequence, the amine could not be attached to the surface of nanoparticles and the amount of defects that are related with blue emission were not formed abundantly. Therefore, the FTIR spectrum of sample T4 had a similar content of impurities and a low blue emission as sample T0. This could explain why the luminescence decreased from T3 to T4. However, the sample T4 synthesized with TEA had stronger integrated emission than T0 see Fig. 3(c). From here, we can assume that the amount of defects produced in T4 should be higher compared to T0. This behavior corroborates that amines provided by TEA and located on the surface of ZnO quantum dots augment the amount of defects, which in turn raises luminescence.

3.4 Origin of defects produced by TEA

According to Fu et al., carboxylate complexes formed by the reaction of hydroxyl and carboxyl groups (COOHs) could be responsible for the blue emission [20]. In our case, we have hydroxyl groups coming from TEA and COOH groups coming from ZnAc (see bands at 1409 cm^{-1} and 1569 cm^{-1} in Fig. 3(d)), then, it can be assumed that our blue emission should be associated to carboxylate groups again. Nevertheless, we prepared one sample using Zinc nitrate instead of ZnAc as source of Zn and we obtained a strong blue emission again, see sample T5 in Fig. 5. This result points out that the blue emission could be produced as a interaction between amines and the surface of ZnO as explained above and carboxylate groups are not essential to produce blue emission.

#232086 - $15.00 USD Received 16 Jan 2015; revised 30 Mar 2015; accepted 5 Apr 2015; published 17 Apr 2015
(C) 2015 OSA

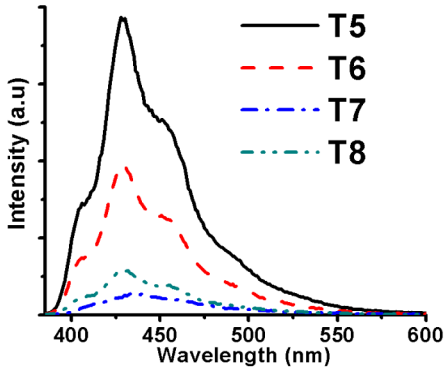

Fig. 5. PL Spectra of samples T5-T8 under 350 nm excitation.

In order to understand how zinc interstitials defects are formed during our synthesis procedure, a solution of TEA and methanol was prepared using the same synthesis conditions of sample T3, after irradiation with 350 nm no emission was observed. Therefore, it is confirmed that the blue emission comes from ZnO nanoparticles. Some authors have reported that the formation and emission of defects in ZnO is caused by the presence of a surfactant or the surface-bonded organic molecules on the surface of nanoparticles, that in turn, are responsible of the creation of surface states that generates visible emission [20,29]. In our case, surfactant is not indispensable to create defects that produce the blue emission because it was observed without the presence of surfactant (TEA), see emission spectra of sample T0 in Fig. 3(a). However, TEA helps to the formation of Zn Interstitial defects since it increased the luminescence of nanoparticles as explained before. M.L. Singla et al. also observed this increase in emission due to an increase in the amount of defects for the green emission of nanoparticles capped with CTAB, TOAB, TEAB and PVP [29]. To understand the role of TEA on the creation such defects, additional samples T5-T8 were synthesized, see Table 2.

Table 2. Synthesis parameters of samples T5-T8.

	Zn Precursor (ml)	Surfactant (ml)	Precipitant	T(°C)
T5	Zinc Nitrate	TEA (1.1ml)	Hexane	60
T6	Zinc Acetate	Hydroxylamine (1.1 ml)	Hexane	60
T7	Zinc Acetate	Oleic Acid (1.1 ml.)	Hexane	60
T8	Zinc Acetate	TEA (1.1 ml.)	NaOH	60

First, it should be demonstrated that the formation of carboxylate groups as result of the reaction between hydroxyl groups provided from TEA and carboxyl groups provided from zinc acetate is not essential for the formation of defects that produce blue emission as affirmed by other authors [20]. For this, the sample T5 was synthesized with Zinc nitrate using the same conditions of synthesis of sample T3, in this way the carboxyl groups (COOH) are not introduced. After photoluminescence characterization, see sample T5 in Fig. 5, a blue band is observed again and it has an integrated intensity 7% lower compared to that for sample T3. This indicates that the formation of carboxylate groups is not the origin of defects for blue emission.

Second, the photoluminescence characterization of the sample T0 synthesized without TEA, showed the same blue band compared to the samples T1-T4. Thus, the creation of defects responsible of blue emission could be due to the thermal treatment of ZnO and to the method of precipitation employed during synthesis. Also, this result indicates that the presence of surfactants it is not necessary to obtain defects after synthesis. TEA contains an amine which is an important factor for the formation of defects, since the emission intensity

#232086 - $15.00 USD Received 16 Jan 2015; revised 30 Mar 2015; accepted 5 Apr 2015; published 17 Apr 2015
(C) 2015 OSA

in sample T3 was 7.5 times higher than that for T0. If this statement is correct, it should be observed the same blue emission in samples synthesized with another surfactant that contains an amine. To confirm this assumption, the sample T6 was fabricated by using the same synthesis procedure of sample T3 but hydroxylamine was used as surfactant. Photoluminescence measurements for the sample T6 showed the same blue band but the overall emission was at about 50% lower than that for the sample T3, see Fig. 5. This quenching in intensity could be associated with the amount of OHs introduced by hydroxylamine, this molecule only has one OH radical bound to the Nitrogen atom. Consequently, the probability for an ammine (which create defects for blue emission) to be attached on ZnO nanoparticles should be less than that for TEA which contains three OH radicals. The following step was the fabrication of another sample under the same conditions of synthesis used for sample T3 but the surfactant was oleic acid which does not contains an ammine (sample T7). After PL measurements in hexane, a weak blue emission with an integrated emission 90% lower than that for sample T3 was observed at 435 nm, see Fig. 5. This shift in the blue emission band from 429 nm to 435 nm when oleic acid is used indicates that other types of defects are formed when surfactants without amines are used. This confirms the role of the amine to produce mainly defects emitting at 429 nm. Thus, amine enhances the amount of surface states (defects) on nanoparticles, which in turn produce blue emission. Further, the hexane precipitant has an important role to form defects: The sample T8 was fabricated using the same conditions of synthesis of sample T3 but sodium hydroxide (NaOH) was used as precipitant agent. The PL spectra of sample T8 showed a weak blue emission at 429 nm, see Fig. 5. This supports the fact that the formation of defects depends on the concentration of OHs on the surface of nanocrystals. It is expected a decrease in the emission intensity because NaOH introduced OHs which would be detrimental for emission, but hexane does not introduce such OHs, facilitating the preservation of defects formed during synthesis. Those results suggest that the formation and preservation of defects is not possible only with presence of TEA or hexane individually during synthesis. Hence, the combined presence of TEA and hexane produces and preserves more defects than these ones produced by the solely presence of TEA or hexane.

3.5 Quantum yield

The quantum yield (QY) is defined as the ratio of emitted photons to absorbed excitation photons. In this work, the QY of ZnO quantum dots dispersed in hexane was obtained by using a comparative method which required the quinine sulfate dye (QS) as a reference [20]. We calculated the QY for the sample T3 which had the highest emission intensity. Basically, it was calculated by comparing the integrated photoluminescence intensities (excited at 350 nm) and the absorbency values (at 350 nm) of the ZnO QDs with the reference quinine sulfate, see Fig. 6. Five solutions with different concentrations of each compound were prepared and all of them had absorbance values less than 0.1 at 350 nm. To prepare those solutions, ZnO quantum dots were dispersed in hexane (refractive index of hexane $\eta_{ZnO} = 1.375$) and QS was dissolved in a aqueous solution 0.5M of sulfuric acid (H_2SO_4) (refractive index of aqueous solution $\eta_{QS} = 1.33$). The QY was calculated using the following equation: $QY = QY_{QS}(0.55)(m_{ZnO}/m_{QS})(\eta_{ZnO}^2/\eta_{QS}^2)$, where QY_{QS} is the quantum yield of the quinine sulfate dye (0.55), m is the gradient (linear slope) from the plot of integrated photoluminescence intensity versus absorbance, η_{ZnO} and η_{QS} are the refractive index of hexane and quinine sulfate respectively. From this equation, a value of QY = 81% was obtained for sample T3. This result indicates that TEA is very effective to increase the efficiency of blue emission in ZnO quantum dots, even more than oleic acid which helps to produce blue emission with a quantum yield of 76% in water [20]. The intensity of light generated by ZnO nanoparticles is related with the content of defects in this material, then, it is expected a higher emission intensity and quantum yield as the content of defects increases. The type of defect is also related with the efficiency for the generation of blue light.

#232086 - $15.00 USD Received 16 Jan 2015; revised 30 Mar 2015; accepted 5 Apr 2015; published 17 Apr 2015
(C) 2015 OSA

Particularly, Zinc interstitial defects are efficient for the generation of blue emission [13,14]. In our case, the presence of amines on the surface of ZnO QDs benefits the generation of blue emission, thus, if we want to increase the QY even more, we have to find alternative methods to increase the presence of amines on the surface of ZnO QDs. Finally, all those results demonstrate that our nanoparticles could be useful for biolabeling and optoelectronics applications where materials with high QY and photostability are very desirable [41].

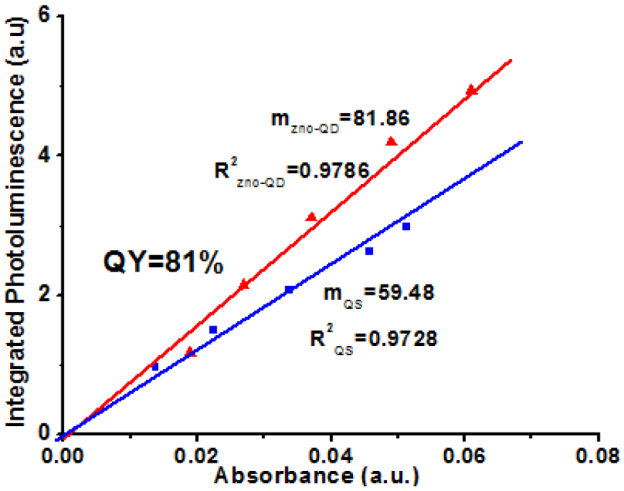

Fig. 6. Fitting used to calculate the quantum yield (QY) of ZnO quantum dots dispersed in hexane. The quinine sulfate dye (QS) was used as a reference.

4. Conclusions

The presence of amines and OH groups was important to increase or decrease surface states or Zn interstitials, which are directly related with the intensity of the blue emission in ZnO quantum dots. As the content of TEA increases the blue emission increases, but after 1.1 ml this emission is quenched because the surface of ZnO quantum dots did not have enough amines, which are related to the formation of defects responsible of blue emission. The energy band gap values (BG) and the size of ZnO quantum dots were controlled by the concentration of TEA. Two methods were used to calculate this band gap and the maximum difference between the values of BG given by both methods was 7%. Finally, the high quantum yield of 81% (respect to QS) for blue emission suggests that those nanoparticles could be useful for applications in biolabeling or optoelectronics devices such as ZnO based LEDs.

Acknowledgments

We acknowledge the financial support from CONACyT through grant 134111 and PhD scholarship for Jorge Oliva and Leonardo Perez.

#232086 - $15.00 USD Received 16 Jan 2015; revised 30 Mar 2015; accepted 5 Apr 2015; published 17 Apr 2015
(C) 2015 OSA